DRAG COEFFICIENTS OF SUPERCAVITATING BODIES OF REVOLUTION AT VARIOUS ANGLES OF YAW

by

Matilde Macagno and Tsu-Ying Hsieh

Institute of Hydraulic Research
University of Iowa
Iowa City

Contract Nonr 1509(05)
Task NR 062-271

March 1963

DRAG COEFFICIENTS OF SUPERCAVITATING BODIES OF REVOLUTION AT VARIOUS ANGLES OF YAW

Introduction

One phase of a study of the drag of supercavitating bodies of revolution consisted of collecting the drag data already available in the literature. In order to supplement the limited data so discovered, the evaluation of the drag coefficients of various head forms under cavitating conditions at various angles of yaw, from the measured values of the pressure distribution, was undertaken.

The aforementioned pressure distributions for zero angle of yaw were published by the Iowa Institute of Hydraulic Research, in 1948 [1]*. Eight of the head forms included in these first tests were selected for a further study of pressure distribution under cavitating conditions at angles of yaw and the results were published in 1962 [2]. The latter also included pressure distribution measurements at zero angle of yaw. The results obtained for the drag coefficients of the various head forms at several yaw angles will be presented and compared with the directly measured values for the drag at zero angle of yaw available in the literature. No data on direct measurements of drag at angles of yaw have been found.

This work was supported by BuShips, Code 421, under Contract Nonr 1509(05), Task NR 062-271.

---

*Numbers in [ ] indicate references at the end of this report.

Nomenclature

d	diameter of the body
g	acceleration of gravity
h	pressure head at a point of the body surface
h_0	pressure head of undisturbed flow
h_c	cavity-pressure head
h_v	vapor-pressure head
$\bar{i}, \bar{j}, \bar{k}$	unit vectors in the x, y, z directions
l, m, n	direction cosines of the normal vector $\bar{n}$
$\bar{n}$	unit vector normal to the surface of the body
p_0	constant pressure of the undisturbed flow
p_c	pressure in cavity
r	radius of transverse section of a body of revolution
s	arc length measured from nose along a meridian section
s_1, s_2	arc lengths on the lee ($\theta = 0$) and windward ($\theta = \pi$) sides measured to the points at which cavitation begins
u_0	axial component of incident flow
u_s	velocity component tangent to the arc of a meridian section
u_θ	velocity component tangent to the circle of a transverse section
v_0	transverse component of incident velocity
x, y, z	Cartesian coordinates
x, r, θ	cylindrical coordinates
x_s	abscissa of the stagnation point
A_b	maximum or base area of section of the body
A_c	area of transverse section at s_2

C_D drag coefficient

C_{D1}, C_{D2}, C_{D3}, C_{D4} drag coefficients due to pressures on various zones of body

C_p pressure coefficient

C_{p_1} C_{p_2} pressure coefficients on the lee and windward sides of the body

D drag

$\bar{F}$ force acting on the body

$G(x)$ equation of the body, $r^2 = G(x)$

K_c cavitation number based on cavity pressure

K_v cavitation number based on vapor pressure

V_0 magnitude of incident velocity

α angle of yaw

β a coefficient

γ angle defined by $\sin\gamma = dr/ds$

Δp difference between pressure on the surface of the body and that in the undisturbed flow

$\Delta p'$ difference between the cavity pressure and that in the undisturbed flow

$\theta_c(s)$ azimuthal angle at which cavitation begins

ρ mass density

Analysis of Pressure Data at Zero Angle of Yaw

We will employ cylindrical coordinates (x, r, θ) with the x-axis along the axis of symmetry and the origin at the nose of the body. The bodies for which the drag coefficients are analyzed consist of heads of the shape of a body of revolution. The equations of these surfaces are expressible in the form

$$y = r(x)\cos\theta \quad , \quad z = r(x)\sin\theta$$

These equations also relate the cylindrical with the rectangular coordinates (x, y, z) which will be convenient to use in some parts of this report. The slope at any point of the surface is given by

$$\tan\gamma = \frac{dr}{dx}$$

See Figs. 1 and 2.

In reference [1], the cavitation number, K_v, was based on vapor pressure,

$$K_v = \frac{h_0 - h_v}{V_0^2/2g} \tag{1}$$

where h_0 is the pressure head of the undisturbed flow, h_v is the vapor-pressure head, V_0 is the velocity of the undisturbed flow, and g is the acceleration of gravity. It was found, however, that the cavity pressure was always higher than the vapor pressure, probably because of the presence of air in the cavity. Therefore, in evaluating the drag coefficient, it seems to be more reasonable to use a cavitation number which is based on the cavity pressure, K_c [3]

$$K_c = \frac{h_0 - h_c}{V_0^2/2g} \tag{2}$$

in which h_c is the cavity-pressure head.

It will be assumed that the pressure distribution over the portion of the supercavitating body immersed in the cavity is constant and equal to the cavity pressure. The drag D is then given by

$$D = \int_S \Delta p \, dA_b - A_b \Delta p' \tag{3}$$

where Δp is the difference between the pressure on the surface of the body and that in the undisturbed flow, $\Delta p'$ is the difference between the cavity pressure and that in the undisturbed flow, D is the drag of the body, A_b is the area of the body projected on a plane perpendicular to its axis of symmetry, and the integral in (3) extends over the surface of the body.

Defining the drag coefficient C_D and the pressure coefficient C_p by

$$C_D = \frac{D}{(1/2)\rho V_0^2 A_b} \qquad\qquad C_p = \frac{h - h_0}{V_0^2/2g} \tag{4}$$

where h is the pressure head at a point of the body surface, we readily obtain from (3)

$$C_D = 4\int_0^{r_b} C_p \, d\left(\frac{r}{d_b}\right)^2 + K_c \tag{5}$$

in which r is the radius of the body at a transverse section and d_b the maximum diameter of the body.

In (5), the integral can be evaluated by graphical integration over the area under the C_p - vs - $(r/d_b)^2$ curve. Values of C_p , K_c and (r/d_b) were obtained from references [1] and [2], and the area was measured both by means of a planimeter and numerically by using Simpson's quadrature rule.

Analysis of Pressure Data at Angles of Yaw

If the flow is assumed to be irrotational and the fluid inviscid and incompressible, and if a stream of velocity V_0 is incident on a body of revolution at an angle of incidence α with the x-axis, the velocity field may be obtained by superposition of an axial flow $u_0 = V_0 \cos\alpha$ and a transverse flow $v_0 = V_0 \sin\alpha$; see Fig. 3.

The force acting on the body is given by the integral over the surface of the body

$$\bar{F} = -\int_S p\,\bar{n}\,dS$$

where $\bar{n}$ is the unit vector normal to the surface of the body

$$\bar{n} = \bar{i}\,l + \bar{j}\,m + \bar{k}\,n$$

expressed in terms of unit vectors $\bar{i}$, $\bar{j}$, $\bar{k}$ in the direction of the x, y, and z axes. Defining the drag D as the component of $\bar{F}$ in the direction of the flow, we have

$$D = \bar{F}\cdot(\bar{i}\cos\alpha + \bar{j}\sin\alpha) = \int_S p\,(l\cos\alpha + m\sin\alpha)\,dS$$

From the equation of the body of revolution

$$r^2 - G(x) = 0 \quad , \qquad r^2 = y^2 + z^2 \tag{6}$$

one obtains the direction cosines of the normal vector $\bar{n}$

$$-\frac{G'}{\sqrt{G'^2 + 4r^2}} \quad , \quad \frac{2y}{\sqrt{G'^2 + 4r^2}} \quad , \quad \frac{2z}{\sqrt{G'^2 + 4r^2}}$$

in which $G' = dG/dx$. Also we have

$$dS = r\,d\theta\,ds \quad , \qquad ds = \sec\gamma\,dx$$

Hence the expression for the drag becomes

$$D = \iint r\,p\,\frac{G'\cos\alpha - 2y\sin\alpha}{\sqrt{G'^2 + 4r^2}}\,d\theta\,ds$$

On introduction of $G' = 2r \tan \gamma$, the following expression for D is obtained

$$D = \iint r\, p\,(\sin\gamma \cos\alpha - \cos\gamma \sin\alpha \cos\theta)\, d\theta\, ds \tag{7}$$

The force on the body due to a constant pressure p_0 is zero:

$$0 = \iint r\, p_0\,(\sin\gamma \cos\alpha - \cos\gamma \sin\alpha \cos\theta)\, d\theta\, ds$$

Subtracting this equation from D and dividing by $1/2\, \rho\, V_0^{\,2} A_b$ yield the following expression for C_D :

$$C_D = \frac{1}{A_b} \iint r\, C_p (\sin\gamma \cos\alpha - \cos\gamma \sin\alpha \cos\theta)\, d\theta\, ds \tag{8}$$

If the pressure distribution were known over the entire surface of the body, the drag could be obtained from (8). Unfortunately, the only pressure measurements available [2] are for a single meridian plane, for $\theta = 0$ and π . Nevertheless, by introducing a reasonable but approximate assumption, it has been possible to evaluate the drag coefficient from the integral (8).

The nature of this assumption will be better comprehended by first recalling certain relations between the velocity components for fully wetted potential flow about a body of revolution. Denote the velocity distribution along the surface of the body, corresponding to the axial flow u_0 , by $u_0 f(x)$. In accordance with the theory of transverse flows on a body of revolution [4], the velocity distribution corresponding to v_0 consists of the components $v_0 g(x) \cos \theta$ along the arc of the meridian section and $v_0 h(x) \sin \theta$ in the direction of increasing θ . The resultant velocity components at a point (x, r, θ) of the body are then of the form

$$u_s = V_0 \left[f(x) \cos\alpha + g(x) \sin\alpha \cos\theta \right] \tag{9}$$

$$u_\theta = V_0\, h(x) \sin\alpha \sin\theta \tag{10}$$

where, by [4], $g(x)$ and $h(x)$ are related by

$$g(x) = -\frac{d}{ds}\left[r\,h(x)\right] \tag{11}$$

Here u_s is the resultant velocity component tangent to the arc of a meridian section and u_θ is the velocity component tangent to the circle of a transverse section; see Fig. 4.

The assumption can now be stated, that over the fully wetted portion of a supercavitating body of revolution at an angle of yaw, the variation of the velocity components u_s and u_θ with the aximuthal angle θ is in accordance with (9), (10) and (11). This assumption is not exact, since the total stream surface bounded by the head form and the free streamlines is not a surface of revolution. Nevertheless, it appears reasonable to conclude that the deviation from the assumed law will be small over the wetted portion of the body, which is actually a surface of revolution.

The functions $f(x)$ and $g(x)$ can now be obtained from the measured values of the pressure distribution on the upper and lower parts of the vertical meridian. Let

$$C_{p_1} = \frac{p_1 - p_0}{(1/2)\,\rho\, V_0^2} \qquad C_{p_2} = \frac{p_2 - p_0}{(1/2)\,\rho\, V_0^2}$$

denote the pressure coefficients on the upper and lower parts respectively. Then, from the Bernoulli equation, we have

$$C_{p_1} = 1 - \frac{u_s^2 + u_\theta^2}{V_0^2} = 1 - \left[f(x)\cos\alpha + g(x)\sin\alpha\right]^2 \tag{12}$$

and similarly

$$C_{p_2} = 1 - \left[f(x)\cos\alpha - g(x)\sin\alpha\right]^2 \tag{13}$$

Then

$$f(x)\cos\alpha + g(x)\sin\alpha = \sqrt{1 - C_{p_1}} \tag{14}$$

and

$$f(x)\cos\alpha - g(x)\sin\alpha = \begin{cases} +\sqrt{1-C_{p_2}} & , x \geqslant x_s \\ -\sqrt{1-C_{p_2}} & , x \leqslant x_s \end{cases} \tag{15}$$

where x_s is the abscissa of the stagnation point. Hence we obtain

$$f(x)\cos\alpha = \frac{1}{2}\left[\sqrt{1-C_{p_1}} \pm \sqrt{1-C_{p_2}}\right] \tag{16}$$

$$g(x)\sin\alpha = \frac{1}{2}\left[\sqrt{1-C_{p_1}} \mp \sqrt{1-C_{p_2}}\right] \tag{17}$$

At $x = 0$ we obtain from (11)

$$g(0) = -\left[r\frac{dh}{ds} + h\sin\gamma\right]_{s=0} = -h(0) \tag{18}$$

For other values of x, we have

$$h(x) = -\frac{1}{r}\int_0^s g(x)\,ds \tag{19}$$

In terms of the functions f, g, and h, the pressure coefficient at any point (x, r, θ) of the body according to (9) and (10), is given by

$$C_p = 1 - [f(x)\cos\alpha + g(x)\sin\alpha\cos\theta]^2 - [h(x)\sin\alpha\sin\theta]^2 \tag{20}$$

It will be convenient to subdivide the surface of the body into four parts. Let s_1 denote the arc length, measured from the nose of the body to the point at which the free streamline separates from the upper or lee side of the body, and s_2 that at which the free streamline separates from the lower or windward side. Then, from $s = 0$ to s_1, the surface is fully wetted at each section. From s_1 to s_2, the body sections are partly wetted, lying in the cavity in the upper part and wetted in the lower; i.e., if $\theta_c(s)$ defines the line of separation of the cavity, the surface is in the cavity for $|\theta| \leqq \theta_c(s)$ and wetted for values $\theta_c(s) \leqslant \theta \leqq \pi$. For $s > s_2$ the body sections lie entirely within the cavity.

For two of these four zones the pressure distribution is either immediately known or readily obtained. Thus, in the fourth zone $(s > s_2)$, we have $C_p = -K_c$, and for the first zone C_p is given by (20) in terms of the values of f and g from (16) and (17). For the third and fourth zones $(s_1 < s < s_2)$ the only data available are the values of C_{p_2}, and it is necessary to make an additional assumption in order to determine the pressure distribution. When the interval s_1 to s_2 is small, as was the case for the bodies which were analyzed in the present work, the error due to the additional assumption, introduced in the following, should also be small.

Substituting in (8) the expression (20) for C_p yields for the integral over the wetted parts of the surface

$$C_D = \frac{1}{A_b}\iint r\left[1-(f\cos\alpha + g\sin\alpha\cos\theta)^2-(h\sin\alpha\sin\theta)^2\right]\left[\sin\gamma\cos\alpha - \cos\gamma\sin\alpha\cos\theta\right]d\theta\, ds \qquad (21)$$

which can be integrated with respect to θ. This gives for C_{D1} and C_{D2}

$$C_{D1} = \frac{1}{A_b}\int_0^{s_1}\left\{\sin\gamma\left[2-2f^2\cos^2\alpha-(g^2+h^2)\sin^2\alpha\right]+2fg\sin^2\alpha\cos\gamma\right\} r\cos\alpha\, ds \qquad (22)$$

$$\begin{aligned} C_{D2} = \frac{2}{A_b}\int_{s_1}^{s_2} r\Big\{&(\pi-\theta_c)\cos\alpha\sin\gamma(1-f^2\cos^2\alpha-h^2\sin^2\alpha)+ \\ &+\sin\theta_c\sin\alpha\left[(1-f^2\cos^2\alpha-h^2\sin^2\alpha)\cos\gamma+2fg\cos^2\alpha\sin\gamma\right] \\ &+\sin^2\alpha\cos\alpha\left[2fg\cos\gamma-(g^2-h^2)\sin\gamma\right]\left(\frac{\pi-\theta_c}{2}-\frac{1}{4}\sin 2\theta_c\right) \\ &-(g^2-h^2)\sin^3\alpha\left(\sin\theta_c-\frac{1}{3}\sin 3\theta_c\right)\cos\gamma\Big\}\, ds \end{aligned} \qquad (23)$$

Since the value $C_p = -K_c$ is assumed within the cavity, the surface integral (8) yields for the third and fourth zones

$$C_{D3} = \frac{2K_c}{A_b}\int_{s_1}^{s_2} r\,(\theta_c \cos\alpha \sin\gamma - \sin\theta_c \sin\alpha \cos\gamma)\, ds \tag{24}$$

$$C_{D4} = \frac{A_c}{A_b} K_c \cos\alpha \tag{25}$$

where A_c is the area of transverse section at s_2. The total drag coefficient is now given by

$$C_D = C_{D1} + C_{D2} + C_{D3} + C_{D4} \tag{26}$$

The additional assumption mentioned above is needed for the evaluation of the functions $f(x)$, $g(x)$, and $h(x)$ in the interval $s_1 \leq s \leq s_2$, on which C_{D2} depends. The assumption introduced is that θ_c, the aximuthal angle at which cavitation begins, changes linearly from 0 to π with arc length s, as s changes from s_1 to s_2; i.e.,

$$\theta_c = \pi \, \frac{s - s_1}{s_2 - s_1} \tag{27}$$

We also have from (20) and (15)

$$[f(x)\cos\alpha + g(x)\sin\alpha\cos\theta_c]^2 + h^2(x)\sin^2\alpha\sin^2\theta_c = 1 + K_c \tag{28}$$

$$f(x)\cos\alpha - g(x)\sin\alpha = \sqrt{1 - C_{p_2}} \tag{15}$$

and from (19),

$$r\,h(x) - r_1 h(x_1) = -\int_{s_1}^{s} g(x)\, ds$$

where $r_1 = r(x_1)$, and x_1 corresponds to s_1. Evaluating the integral by the trapezoidal rule, assuming the interval s_1 to s_2 to be small, we obtain

$$h(x) = \frac{1}{r}\left\{ r_1 h(x_1) - \frac{1}{2}(s - s_1)\left[g(x) + g(x_1)\right]\right\} \tag{29}$$

The variation of f, g, and h with x or s can now be readily determined from (15), (27), (28), and (29).

An alternative assumption, that was also used, employed values of $f(x)$ extrapolated from its known curve for the wetted portion $0 \leq s \leq s_1$, instead of (27). The values of θ_c, $g(x)$ and $h(x)$ were then obtained from (15), (28) and (29). The difference between the values of C_{D2} in (23) obtained by these alternative procedures was negligible.

Results

Curves of C_D vs K_c for various head forms at zero angle of yaw are shown in Fig. 6.

Values of C_{p_1} and C_{p_2} were obtained from reference [2] and the drag coefficient was computed for the cases in which the data showed that a steady cavitation bubble was present. It appeared to be possible to evaluate C_D for only the following forms: the hemispherical, the 2-caliber ogival, the 45°-conical and 2:1 ellipsoidal heads.

The above-described method was applied to the hemispherical and ogival heads. For the conical and ellipsoidal heads, no partly cavitating zone needed to be considered. Typical curves for f, g, and h are plotted against s/d for the hemispherical head in Fig. 5. The calculations for C_D were performed by an IBM 7070 computer.

The resulting values of the drag coefficients are presented in the following table where the values for $\alpha = 0$ are also listed for comparison. The data are also graphed in Fig. 15.

Drag Coefficients of Supercavitating Bodies at Angles of Yaw

	α in deg.	K_c	C_D
hemispherical head	0	0.078	0.349
	0	0.210	0.424
	0	0.300	0.463
	6	0.105	0.359
	6	0.280	0.470
	15	0.100	0.359
conical head	0	0.085	0.282
	0	0.155	0.324
	0	0.240	0.377
	6	0.100	0.301
	6	0.300	0.435
	15	0.085	0.294
	15	0.250	0.415
2:1 ellipsoidal head	0	0.105	0.226
	0	0.215	0.280
	6	0.105	0.277
2-caliber ogival head	6	0.105	0.195
	6	0.175	0.218

Discussion

Comparison of values of C_D at zero angle of yaw obtained from the Iowa data and the other available data are shown in Figs. 7 to 13, [5 - 10]. However, the Iowa data are for relatively high values of K_c, while most available data are for relatively low values of K_c. Therefore, a direct comparison of results can only be made between Iowa data and D.T.M.B. data for the hemisphere, the 2:1 ellipsoid, the 2-caliber ogive, and the blunt head. From Figs. 7, 9, and 11 it is seen that the Iowa points are always higher than those from D.T.M.B.; i.e., about 7 percent higher for the blunt, 15 percent higher for the hemisphere, and about 36 percent higher for the 2:1 ellipsoid and the 2-caliber ogive. In absolute magnitude, the differences are of the same order for the blunt and hemispherical heads and somewhat greater for the 2:1 ellipsoid and 2-caliber ogive. This discrepancy in drag coefficient might be due to the fact that the D.T.M.B. model was supported by a sting of small diameter in comparison with the maximum diameter of the head, but the Iowa head was followed by a cylindrical body (see Fig. 14). As is described in reference [7], for relatively large values of K_c there is a vortex flow of a vapor-water mixture behind the model, when supported by a sting, and a reentrant jet. The latter, impinging on the base, would be expected to increase slightly the pressure on it. On the other hand, this phenomenon would not occur with a cylindrical afterbody. The fact that the two sets of data converge with decreasing values of K_c is also in accordance with the foregoing argument, since the effect of the reentrant jet would be expected to diminish with increasing length of cavity. The drag coefficient for the Reichardt models, Figs. 7, 8, 12, which were sting supported, are also smaller than the Iowa values. The results for the Convair heads, which were also attached to cylindrical afterbodies, lie between those for Iowa and D.T.M.B.

As is seen in Fig. 11, the drag coefficient for a sting-supported 2:1-parabolic head at zero cavitation number, obtained both experimentally and theoretically by N.A.S.A. [9], is $C_D = 0.125$. This agrees with the D.T.M.B. result obtained by extending the C_D vs K_c curve to $K_c = 0$. On the other hand, the value obtained by extrapolating the Iowa data is

higher. It is again suggested that this difference may be attributable to the mode of support.

The results for the drag coefficient at 6° and 15° angles of yaw from the data of reference [2], shown in Fig. 15, indicate the following:

1. The drag coefficient C_D increases with increasing cavity pressure K_c, according to a linear law which agrees with that proposed by Eisenberg [10],

$$C_D(K_c) = C_D(0)(1+\beta K_c)$$

for bodies on which the point of detachment varies with K_c, and

$$C_D(K_c) = C_D(0)(1+K_c)$$

for a fixed point of detachment. The constants for each form were found to be slightly different from those given by Eisenberg.

2. The drag coefficient, for a given value of the cavitation number, appears to increase slightly with the angle of yaw.

3. The relative order of increasing drag coefficients for different head forms for $\alpha = 6^{\circ}$, shown in Fig. 14d, is as follows: (1) ogive, (2) ellipsoid, (3) cone, (4) hemisphere.

Conclusions and Recommendations

From the foregoing study of drag coefficients of bodies of revolution in supercavitating flows at various angles of yaw, the following conclusions were reached:

1. The drag coefficients computed from the Iowa pressure data are higher than the values from other sources. This may depend upon how the head form was supported. The effect of the mode of support should be studied.

2. A linear relationship between C_D and K_c has been confirmed for all the head forms, even at relatively high cavitation numbers. The slope of each straight line varies slightly.

3. Only a slight change in the drag coefficient was found when the body was subjected to angles of yaw of 6 and 15 degrees in supercavitating flows.

Direct measurements of the drag of cavitating head forms at angles of yaw are lacking and should be undertaken.

Acknowledgment

The authors are very grateful to Professor L. Landweber, under whose direction this research was performed, for his valuable advice and suggestions.

References

1. Rouse, H., and McNown, J. S., "Cavitation and Pressure Distribution - Head Forms at Zero Angle of Yaw," Bulletin 32, Studies in Engineering, University of Iowa, 1948.

2. Rouse, H., "Cavitation and Pressure Distribution - Head Forms at Angles of Yaw," Bulletin 42, Studies in Engineering, University of Iowa, 1962.

3. "Tests of a Cavitating Hydrofoil," Final Report, Contract N9onr-93805 under BuShips Hydromechanics Research Program, Iowa Institute of Hydraulic Research, 1961.

4. Landweber, L., "Potential Flow About Bodies of Revolution and Symmetric Two-Dimensional Forms," ONR Report, Iowa Institute of Hydraulic Research, 1959.

5. Reichardt, H., "The Laws of Cavitation Bubbles at Axially Symmetrical Bodies in a Flow," Reports and Translations, No. 166, Ministry of Aircraft Production, August 1946.

6. Oversmith, R. H., "Some Observations on Cavitating Flows," Report No. 2R-659-015, Engineering Department, Convair, 1959.

7. Eisenberg, P., and Pond, H. L., "Water-Tunnel Investigations of Steady-State Cavities," TMB-Report 668, 1948.

8. Plesset, M., and Shaffer, P., "Cavity Drag in Two and Three Dimensions," Journal of Applied Physics 19, 934-939, 1948.

9. Cox, R. N., and Maccoll, J. W., "Recent Contributions to Basic Hydroballistics," Chap. IX of Symposium on Naval Hydrodynamics, Edited by F. S. Sherman, Publication 515, National Academy of Sciences - National Research Council, 1957.

10. Johnson, V. E., and Rasnick, T. A., "The Drag Coefficient of Parabolic Bodies of Revolution Operating at Zero Cavitation Number and Zero Angle of Yaw," Technical Report R-86, N.A.S.A., 1961.

11. Eisenberg, P., "A Brief Survey of Progress on the Mechanics of Cavitation," TMB-Report 842, 1953.

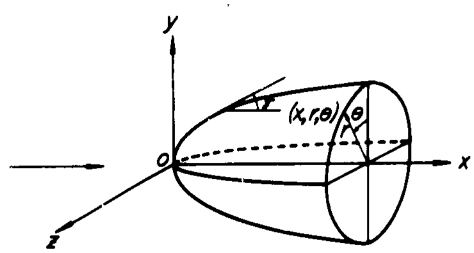

Fig. 1. Sketch of body of revolution

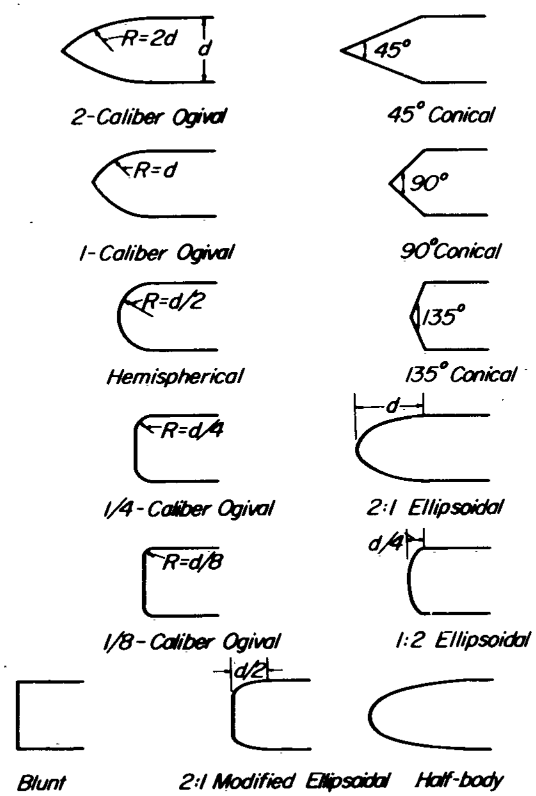

Fig. 2a. Head forms studied at zero angle of yaw

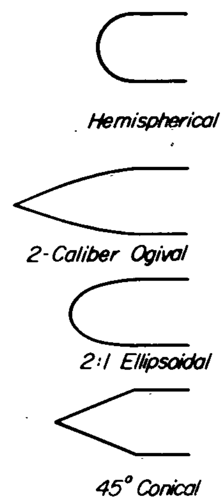

Fig. 2b. Head forms studied at various angles of yaw

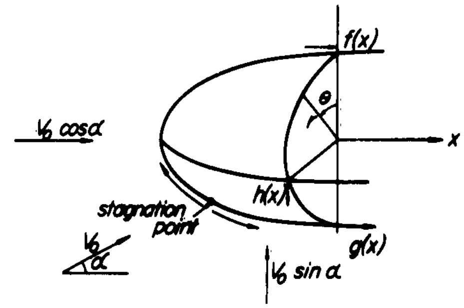

Fig. 3. Velocity components for flow incident at an angle of yaw

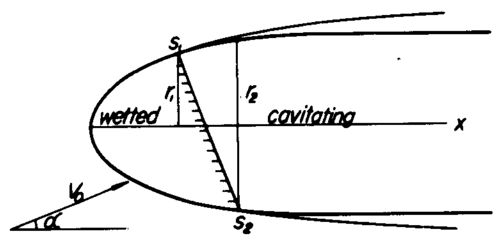

Fig. 4. Sketch showing wetted and cavitating zones

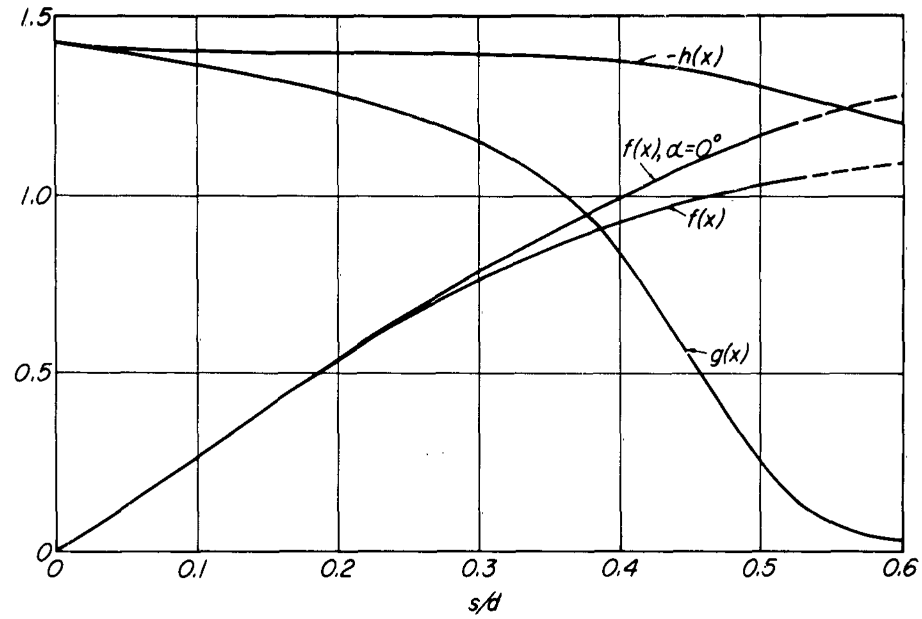

Fig. 5. Auxiliary functions for calculating velocity distribution at an angle of yaw for a hemispherical head. $\alpha = 6°$, $K_c = 0.105$

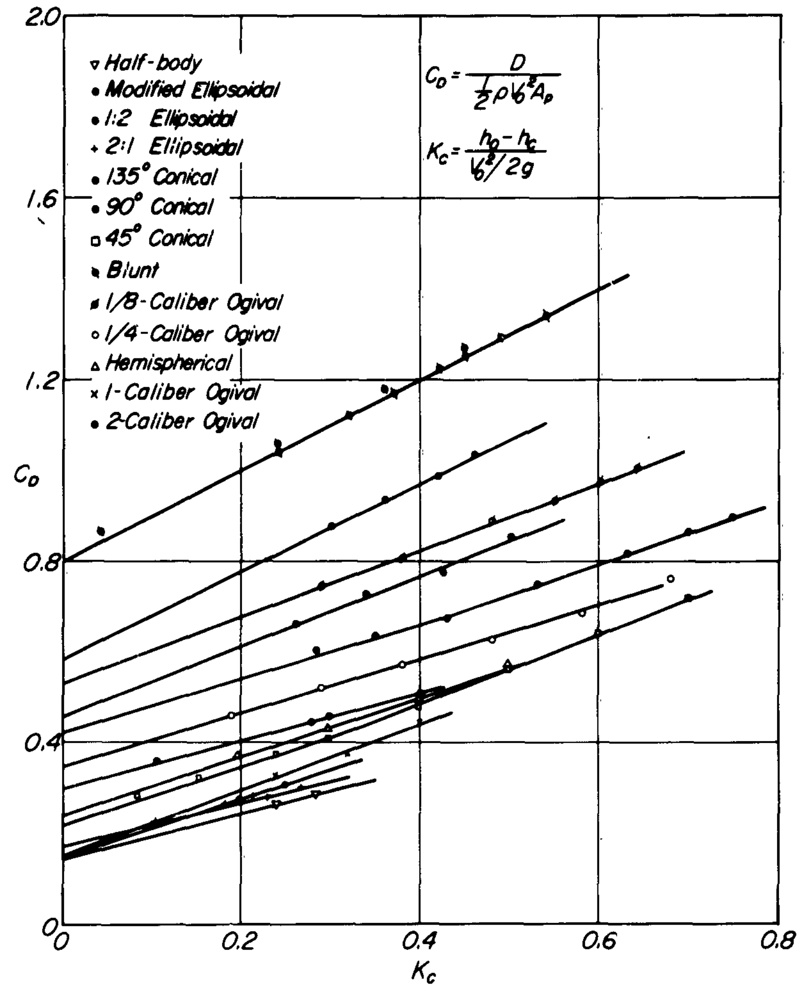

Fig. 6. Drag coefficients for cavitating head forms at zero angle of yaw

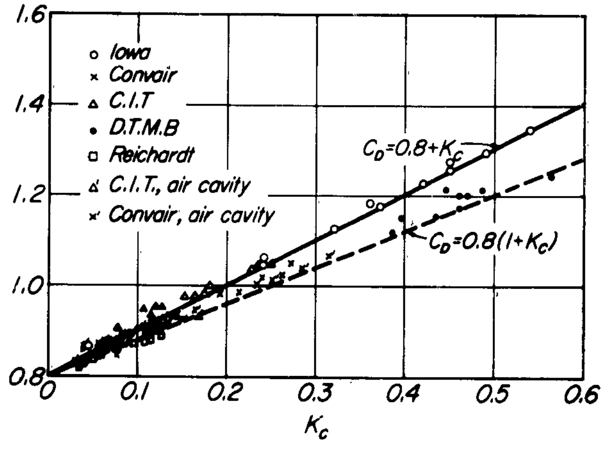

Fig. 7. Drag coefficients for a cavitating blunt head at zero angle of yaw

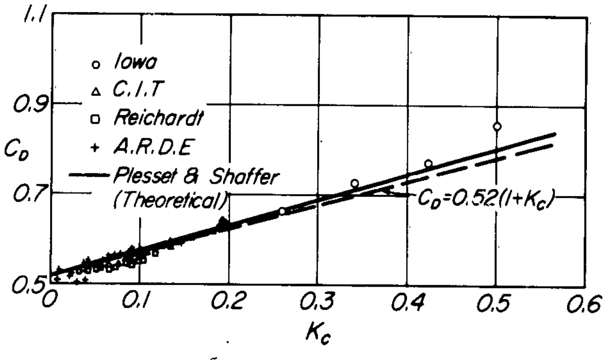

Fig. 8. Drag coefficients for a cavitating 90° conical head at zero angle of yaw

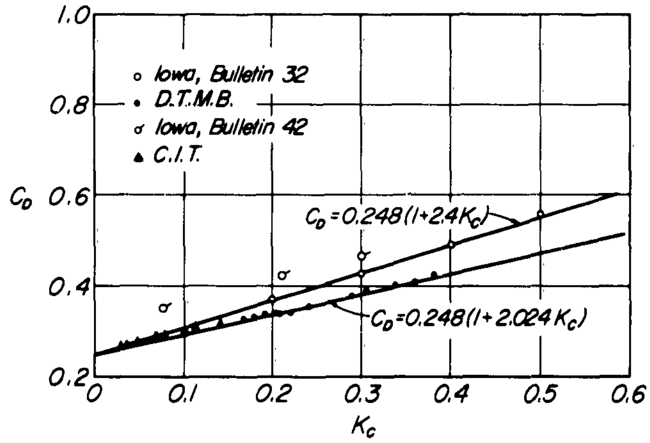

Fig. 9. Drag coefficients for cavitating hemispherical head at zero angle of yaw

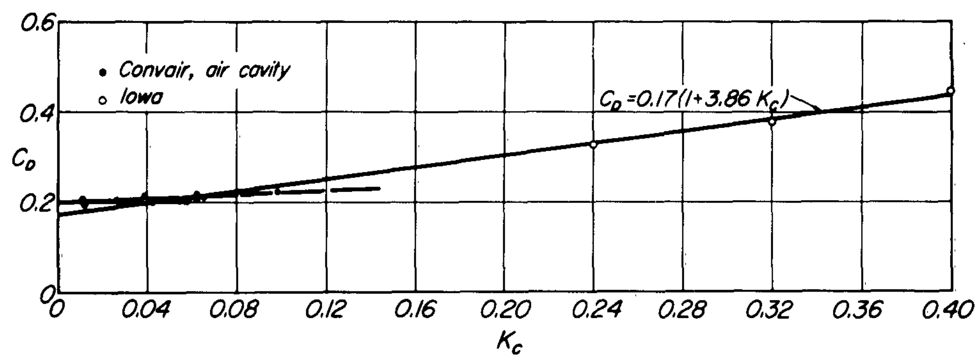

Fig. 10. Drag coefficients for cavitating 1-caliber ogival head at zero angle of yaw

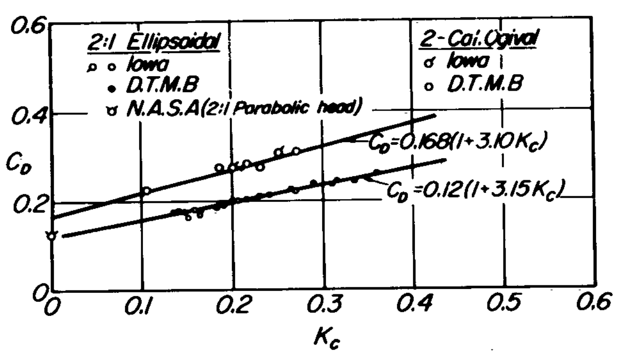

Fig. 11. Drag coefficients for cavitating 2:1 ellipsoidal and 2-caliber ogival heads at zero angle of yaw

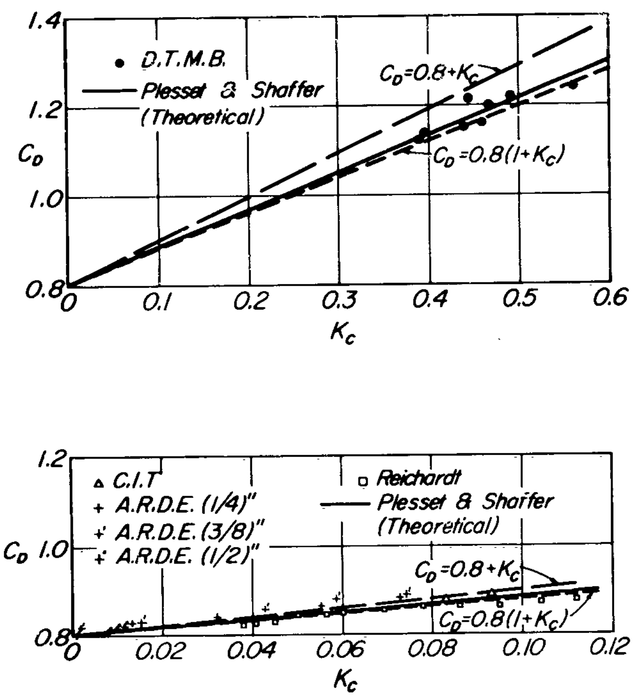

Fig. 12. Drag coefficients for a cavitating disk at zero angle of yaw

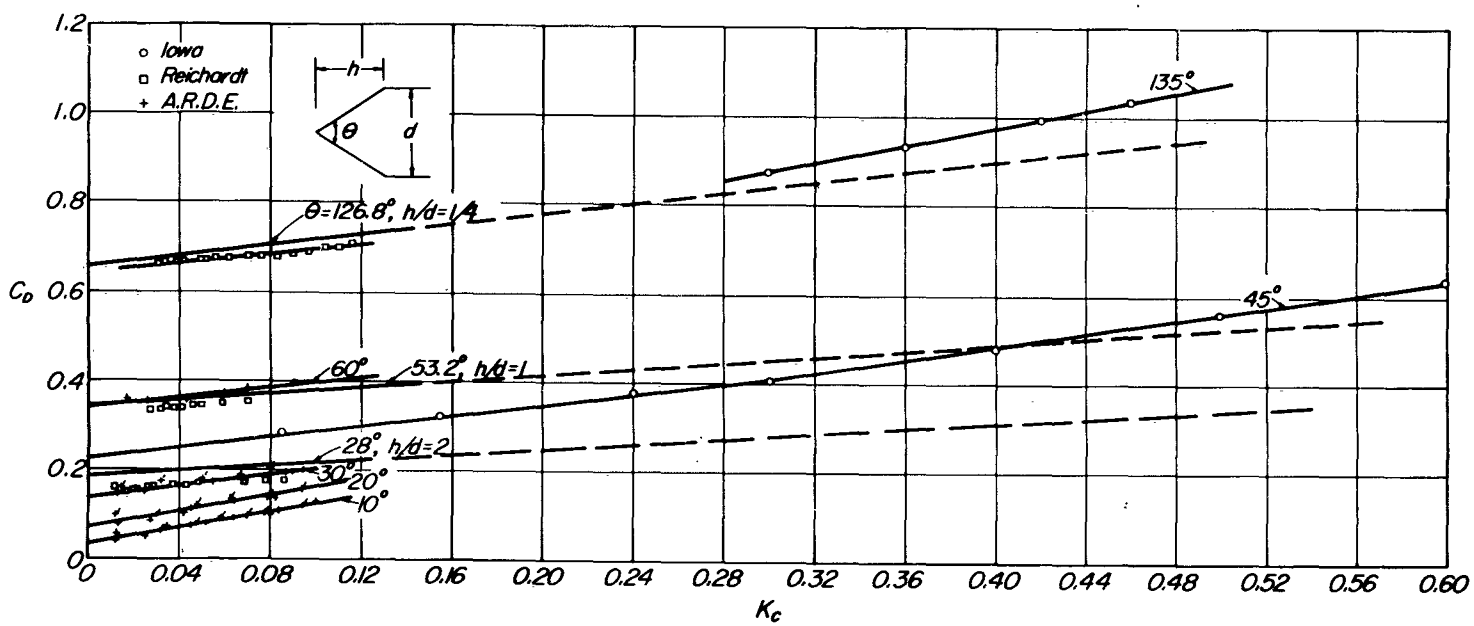

Fig. 13. Drag coefficients for cavitating conical heads at zero angle of yaw

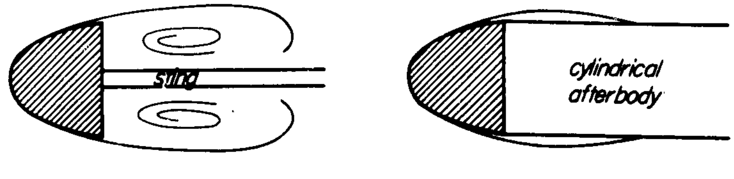

Fig. 14. Sketch of supercavitating flow with different head supports

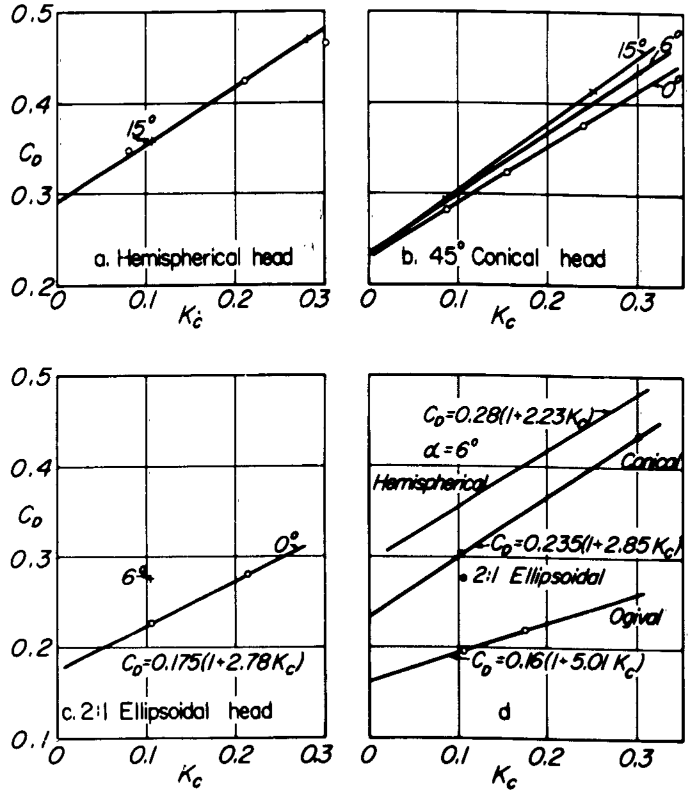

Fig. 15. Drag coefficients of various cavitating heads at angles of yaw